

Relative gain array and singular value decomposition in determination of PSS location

Ali Karimpour^{1,2,*†}, R. Asgharian² and O. P. Malik¹

¹*Department of Electrical Engineering, University of Calgary, Canada*

²*Department of Electrical Engineering, Ferdowsi University of Mashhad, P.O. Box 91775-11 11, Mashhad, Iran*

SUMMARY

In a multi-machine power system, it is important to determine the best location for the application of power system stabilizers. A number of techniques have been proposed to perform this selection. In this paper a new selection measure based on relative gain array and singular value decomposition is proposed. A comparison is made between the performance of the new measure and the older methods. The proposed methodology is based on the use of system transfer function. Copyright © 2005 John Wiley & Sons, Ltd.

KEY WORDS: singular value decomposition; relative gain array; power system stabilizer; controllability; observability

1. INTRODUCTION

Most available control designs assume that a control structure is given at the outset, but one of the first steps for an engineer is to determine the variable that should be controlled, the variable that should be measured, and the input that should be manipulated. An important task in the design of a control system is the specification of the control structure, referred to as control structure design. This leads to closing the gap between theory and application in this area [1,2]. Relative gain arrays (RGA), singular value decomposition (SVD) [3], partial relative gains (PRG) [4] and closed loop interaction number (CLIN) [5] have been introduced as measures of control structure design.

In power systems, several techniques have been proposed in the literature to determine the best location for applying power system stabilizers. The participation factor method is one of the methods for detecting the contribution of various generators in each mode and for suitable location for applying the PSSs [6]. Some authors have proposed the sensitivity of PSS effect (SPE) as a measure for determining the suitable location of PSSs [7]. Modal controllability and modal observability is also considered as a measure for determining the suitable location of PSSs and suitable signal as input of PSSs [8,9]. The relationship among the most popular techniques for identifying a suitable location for applying PSSs is given in Reference [10]. For the selection of the best position for applying static var

*Correspondence to: Ali Karimpour, Department of Electrical Engineering, Ferdowsi University of Mashhad, P.O. Box 91775-11 11, Mashhad, Iran.

†E-mail: karimpour@ferdowsi.um.ac.ir

compensators, residue has been used as a screening measure and final selection has been done with relative gain array [11]. RGA is used as a measure for the selection of suitable locations of stabilizers [12].

Singular value decomposition has been proposed as a measure of the distance of a controllability and observability matrix from singularity in a state space model [8,9]. This distance is used as a measure to compare the ability of inputs to control an oscillation mode.

The main drawback of the above approaches is the determination of linear models from the state space models that usually have large dimensions. Some authors have used the transfer function approach to locate the PSSs. In Reference [13] the peak of transfer function elements in the frequency domain is used as a measure. Transfer function residues are used in Reference [14] to locate PSSs. The singular value is used as a measure to determine the suitable signal for PSSs and their locations in References [15–18].

Surprisingly, the use of RGA and SVD in conjunction with power systems seems to be new, or at least has not been clearly exploited. In this paper the mathematical consideration of RGA and SVD is used for control structure design in power systems. The relationship between measures based on SVD and methods based on controllability measure, observability measure and residue are introduced as well. In this paper only the transfer function of a system is used and thus there is a large reduction in the size of the involved matrices.

The paper is organized as follows: RGA and SVD are described in Sections 2 and 3, respectively; application of the new measures in a power system is described in Section 4; the relationship of results based on SVD and controllability, observability and residue methods is given in Section 5; and the application of RGA and SVD in multi-machine power systems is described in Section 6.

2. RELATIVE GAIN ARRAY

The relative gain array of an $l \times m$ matrix \mathbf{G} is defined as

$$RGA(\mathbf{G}) = \Lambda(\mathbf{G}) = \mathbf{G} \times (\mathbf{G}^\dagger)^T \quad (1)$$

where \mathbf{G}^\dagger is the pseudo inverse of \mathbf{G} , $(\cdot)^T$ means the transpose and \times denotes element by element multiplication. The RGA has a number of interesting control properties, of which the most important ones are [3]:

- For a non-singular square matrix \mathbf{G} , $RGA(\mathbf{G})$ is independent of input and output scaling. For a full row rank matrix, it is independent of output scaling, and for a full column rank matrix, it is independent of input scaling.
- The sum norm of the RGA matrix is very close to the minimized condition number γ^* . This means that plants with large RGA elements are always ill-conditioned.
- The RGA of a matrix can be used to measure diagonal dominance, by the simple equality

$$RGA_{No} = \|\Lambda(\mathbf{G}) - \mathbf{I}\|_{\text{sum}} \quad (2)$$

For decentralized control to avoid instability caused by interaction in the crossover, one should prefer pairing for which the RGA number at crossover frequency is close to zero. Also, to avoid instability caused by interactions at low frequency, one should avoid pairing with negative steady state RGA elements.

- RGA elements imply sensitivity to element-by-element uncertainty. The non-singular and square matrix \mathbf{G} becomes singular if one makes a relative change $1/\lambda_{ij}$ in the ij -th element of \mathbf{G} . That is, if a single element in \mathbf{G} is perturbed from g_{ij} to g'_{ij} in Equation (3), then \mathbf{G} becomes singular:

$$g'_{ij} = g_{ij} \left(1 - \frac{1}{\lambda_{ij}} \right) \tag{3}$$

So a large λ_{ij} means that with a small change in g_{ij} , \mathbf{G} becomes singular.

- The i -th row sum of the RGA is equal to the square of the i -th output projection, and the j -th column sum of the RGA is equal to the square of the j -th input projection as below:

$$\sum_{j=1}^m \lambda_{ij} = \|\mathbf{e}_i^T \mathbf{u}_r\|_2^2 \quad \sum_{i=1}^l \lambda_{ij} = \|\mathbf{e}_j^T \mathbf{v}_r\|_2^2 \tag{4}$$

where $\mathbf{e}_i = [0, 0, \dots, 1, \dots, 0]^T$ is a vector with a 1 in position i and zeros elsewhere; \mathbf{u}_r , and \mathbf{v}_r , respectively, are the output and input directions with non-zero gains extracted from singular value decomposition.

3. SINGULAR VALUE DECOMPOSITION

Consider \mathbf{M} is a constant matrix in $C^{l \times m}$. Then \mathbf{M} can be decomposed into its singular value decomposition according to the following theorem [8].

Theorem. Let $\mathbf{M} \in C^{l \times m}$. Then there exist $\mathbf{\Sigma} \in R^{l \times m}$ and unitary matrices $\mathbf{U} \in C^{l \times l}$ and $\mathbf{V} \in C^{m \times m}$ such that

$$\mathbf{M} = \mathbf{U} \mathbf{\Sigma} \mathbf{V}^C \tag{5}$$

where $\mathbf{\Sigma} = \begin{bmatrix} \mathbf{S} & \mathbf{0} \\ \mathbf{0} & \mathbf{0} \end{bmatrix}$, $\mathbf{S} = \text{diag}\{\sigma_1, \sigma_2, \dots, \sigma_r\}$ with $\sigma_1 \geq \sigma_2 \geq \dots \geq \sigma_r$ and $r \leq \min\{l, m\}$ $\mathbf{U} = [\mathbf{u}_1, \mathbf{u}_2, \dots, \mathbf{u}_l]$, $\mathbf{V} = [\mathbf{v}_1, \mathbf{v}_2, \dots, \mathbf{v}_m]$ and \mathbf{V}^C is the complex conjugate transpose of \mathbf{V} . The column vector elements of \mathbf{U} , identified by \mathbf{u}_i , are orthogonal and of unit length, and represent the output directions. The column vector elements of \mathbf{V} , identified by \mathbf{v}_i , are orthogonal and of unit length, and represent the input directions [3]. These input and output directions are related through singular values. So one can write:

$$\mathbf{M} \mathbf{v}_i = \sigma_i \mathbf{u}_i \tag{6}$$

It means that if an input is applied in the direction \mathbf{v}_i , then the output is in the direction \mathbf{u}_i and has a gain of σ_i . The input direction \mathbf{v}_i for $i > r$ corresponds to inputs that do not have any influence on outputs and similarly output direction \mathbf{u}_i for $i > r$ corresponds to the outputs that cannot be accessed by any input. Since the diagonal elements of \mathbf{S} are arranged in a descending order, it can be shown that the largest gain for any input direction is equal to the maximum singular value σ_1 and so one can write:

$$\sigma_1 = \max_{\mathbf{d} \neq \mathbf{0}} \frac{\|\mathbf{M} \mathbf{d}\|_2}{\|\mathbf{d}\|_2} = \frac{\|\mathbf{M} \mathbf{v}_1\|_2}{\|\mathbf{v}_1\|_2} \tag{7}$$

where \mathbf{d} is any input signal and $\|\cdot\|_2$ is the Euclidian norm. Expansion of Equation (5) leads to the following equation:

$$\underline{\mathbf{M}} = \sum_{k=1}^r \sigma_k \underline{\mathbf{u}}_k \underline{\mathbf{v}}_k^C \quad (8)$$

4. APPLICATION OF RGA AND SVD MEASURES IN POWER SYSTEMS

To see the applicability of RGA and SVD in power systems, consider that there is one machine connected to an infinite bus as shown in Figure 1. The generator is modelled by a seventh order dynamic set of equations [19]. Parameters of generator, exciter, governor and transmission system, and operating point are given in Reference [17]. The input candidates are: exciter Ex and governor Gov, and the output candidates are: power angle δ , speed of generator ω , terminal voltage U_t , electrical power P_e , generator current I_t , and integral of acceleration power $\int (P_e - P_m)dt$. Power angle is in rad, speed is in rad/s and other outputs are in per unit. Scaling plays an important role in figuring out the best input and output [17]. For scaling variables, the maximum expected deviation from the normal value should be chosen. Here, the expected maximum deviation value for the exciter and governor inputs, for current and power is considered as 1 p.u., for voltage it is 0.5 p.u., for power angle π rad, and for speed $0.01 \omega_0$. Dividing each variable by its maximum value scales all variables.

The transfer function of the system at steady state is:

$$\mathbf{G}_{\text{all}} = \begin{bmatrix} -1.5735 & 0.2669 \\ 0.0000 & 0.0000 \\ 1.9874 & -0.0077 \\ -0.0000 & 1.0000 \\ -0.7506 & 0.9707 \\ -1.0873 & 0.1844 \end{bmatrix}$$

where columns 1 and 2 are the two manipulators, exciter and governor, respectively, and rows 1 to 6 are the candidate measurements: power angle, speed of generator, terminal voltage, electrical power, generator current and integral of acceleration power, in that order. The corresponding RGA matrix and row sums Λ_{Σ} are:

$$\Lambda = \begin{bmatrix} 0.3024 & 0.0006 \\ 0.0000 & 0.0000 \\ 0.5425 & -0.0014 \\ -0.0000 & 0.5495 \\ 0.0107 & 0.4510 \\ 0.1444 & 0.0003 \end{bmatrix} \quad \Lambda_{\Sigma} = \begin{bmatrix} 0.3030 \\ 0.0000 \\ 0.5411 \\ 0.5495 \\ 0.4617 \\ 0.1447 \end{bmatrix}$$

One finds from the row sums of the steady state RGA matrix given in Λ_{Σ} that four outputs (δ, P_e, I_t, U_t) have the largest projections onto the output space of \mathbf{G}_{all} . Of course, for control proposes

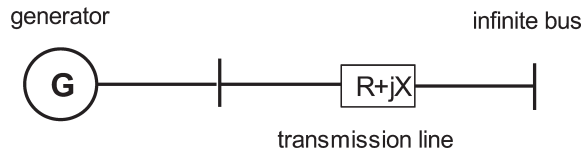


Figure 1. Single machine infinite bus system.

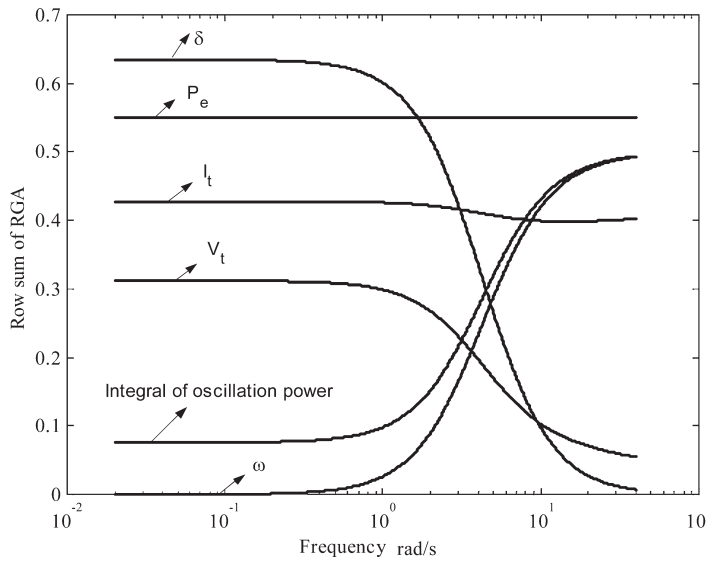


Figure 2. Row sum of RGA matrix.

one must also consider higher frequencies up to crossover. The row sums versus frequency are shown in Figure 2. It shows that the speed of the generator ω (which has no steady state effect), the integral of acceleration power $\int (P_e - P_m)dt$, electric power P_e and generator current I_t are effective at crossover frequency whereas power angle δ and terminal voltage U_t are less effective.

The elements of the RGA matrix for any two choices of the set $\{U_t, \delta, I_t, P_e\}$ versus frequency are shown in Figure 3. Note that the RGA of a 2×2 matrix is symmetric and diagonal elements are equal, so every subplot of Figure 3 has two graphs; the diagonal element is shown by a solid line and the off-diagonal element is shown by a dashed line. Section 2 implies that the RGA matrix near to a unit matrix is preferred. It is seen from Figure 3 that the suitable candidates are $\{(Ex, U_t), (Gov, \delta)\}$, $\{(Ex, U_t), (Gov, P_e)\}$, $\{(Ex, U_t), (Gov, I_e)\}$ and $\{(Ex, U_t), (Gov, P_e)\}$ and the best one is $\{(Ex, U_t), (Gov, P_e)\}$ since its RGA matrix is the nearest one to a unit matrix. One of the four outputs ω, P_e, I_t or acceleration power $\int (P_e - P_m)dt$ must be chosen for higher frequency according to Figure 2.

The above pairing (AVR and governor) is the normal mode of operation in power systems. To improve the system operation, a PSS, effective around the frequency of oscillation, must be added. One of the above signals is used in the PSS to act at the desired frequency through a washout block.

For choosing the best input–output pair for improving the dynamics of the system one must find the SVD of the system at $s = p + \varepsilon$ where p is the oscillation mode of the system and ε is a small value added to p to make $\underline{G}_{all}(s)$ analytical. The SVD is:

$$\underline{G}_{all} \cong 57862 \begin{bmatrix} 0.0848 - 0.0321i \\ 0.0939 + 0.5628i \\ 0.0059 + 0.0080i \\ 0.4271 + 0.0015i \\ 0.4101 - 0.0044i \\ 0.1525 + 0.5406i \end{bmatrix} \begin{bmatrix} 0.9983 \\ 0.0143 - 0.0571i \end{bmatrix}^C$$

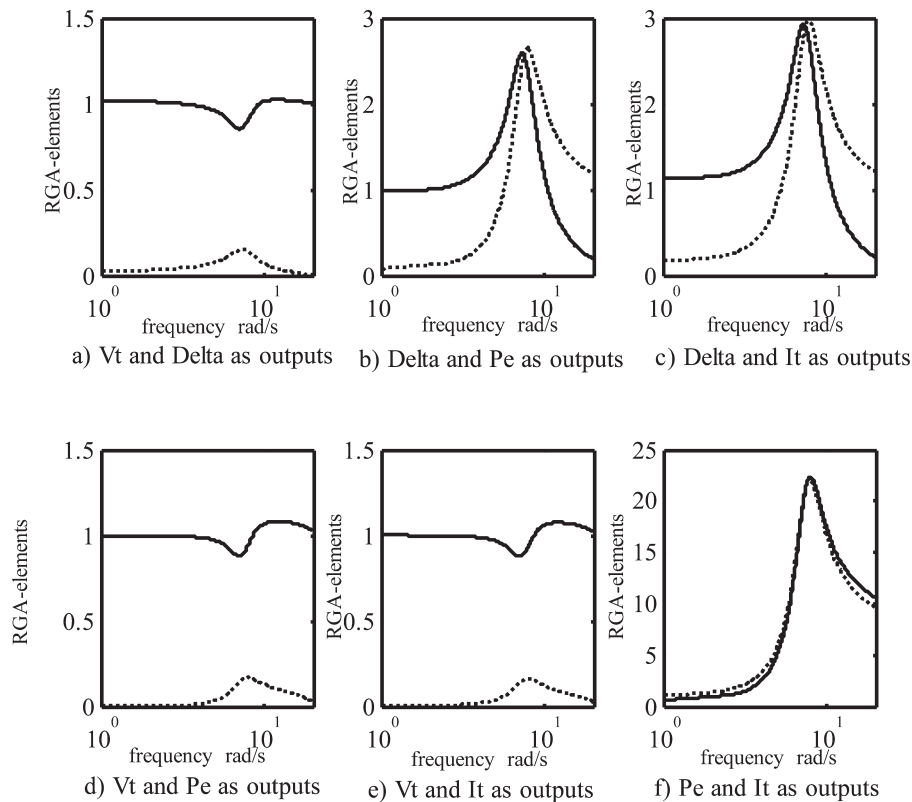


Figure 3. RGA elements for different outputs versus frequency.

Absolute value elements of \underline{u}_1 and \underline{v}_1 are shown by $\hat{\underline{u}}_1$ and $\hat{\underline{v}}_1$ correspondingly:

$$\hat{\underline{u}}_1 = \begin{bmatrix} 0.0907 \\ 0.5706 \\ 0.0100 \\ 0.4271 \\ 0.4101 \\ 0.5617 \end{bmatrix} \quad \hat{\underline{v}}_1 = \begin{bmatrix} 0.9983 \\ 0.0588 \end{bmatrix}$$

The relative magnitude of elements of $\hat{\underline{v}}_1$ shows that the exciter is the most important input and the relative magnitude of elements of $\hat{\underline{u}}_1$ shows that ω is the best signal, after which comes $\int (P_e - P_m)dt$, then P_e , and so on. So one must use ω or $\int (P_e - P_m)dt$ as the measurement signal and apply a suitable signal to the exciter.

5. RELATIONSHIP BETWEEN INDICES BASED ON SVD AND OTHER METHODS

The state equation of the linearized model of a multi-machine power system can be written as:

$$\dot{\mathbf{X}} = \mathbf{A}\mathbf{X} + \mathbf{B}\mathbf{u} \quad (9)$$

$$\mathbf{y} = \mathbf{C}\mathbf{X} \quad (10)$$

where $\mathbf{A} \in R^{m \times m}$, $\mathbf{B} \in R^{m \times n}$, $\mathbf{C} \in R^{p \times m}$, m is the number of states, n is the number of possible inputs and p is the number of possible outputs. If λ_i is the eigenvalue of matrix \mathbf{A} , and $\underline{\varphi}_i$ and $\underline{\psi}_i$ are the corresponding right and left eigenvectors of the state matrix \mathbf{A} with respect to λ_i , then:

$$\mathbf{A}\underline{\varphi}_i = \lambda_i\underline{\varphi}_i \quad (11)$$

$$\underline{\psi}_i^T \mathbf{A} = \underline{\psi}_i^T \lambda_i \quad (12)$$

Right and left eigenvectors are normalized such that:

$$\underline{\psi}_i^T \underline{\varphi}_i = 1 \quad (13)$$

The relative controllability of different inputs on λ_i can be extracted from the corresponding elements of vector $\underline{\mathbf{b}}_i$:

$$\underline{\mathbf{b}}_i = (\underline{\psi}_i^T \mathbf{B})^T \quad (14)$$

where $\underline{\mathbf{b}}_i$ is a vector of dimension $n \times 1$. Its elements indicate how much the i -th mode is excited by different inputs. Relative observability of different outputs on λ_i can be extracted from the corresponding elements of vector $\underline{\mathbf{c}}_i$:

$$\underline{\mathbf{c}}_i = \mathbf{C}\underline{\varphi}_i \quad (15)$$

where $\underline{\mathbf{c}}_i$ is a vector of dimension $p \times 1$. Its elements indicate how much the i -th mode is observed by different outputs. So the large element of $\underline{\mathbf{b}}_i$ corresponds to the more effective input and the large element of $\underline{\mathbf{c}}_i$ corresponds to the more observable output. Thus one can choose the best measured signal and the best inputs.

The residue of λ_i corresponding to different input–output pairs can be extracted from the residue matrix $\underline{\mathbf{R}}$:

$$\underline{\mathbf{R}} = \mathbf{C}\underline{\varphi}_i\underline{\psi}_i^T \mathbf{B} = \underline{\mathbf{c}}_i\underline{\mathbf{b}}_i^T \quad (16)$$

$\underline{\mathbf{R}}$ is a $p \times n$ matrix that considers both controllability and observability together. The largest element of residue matrix corresponds to the best measurement signal and the best input to apply to the controller. Note that because of practical considerations (decentralized controller) the largest diagonal element is preferred. If \mathbf{A} is diagonalizable, the transfer function of the system described by Equations (9) to (10) can be described by the following equation:

$$\underline{\mathbf{G}}(s) = \sum_{i=1}^m \frac{1}{s - \lambda_i} \underline{\mathbf{c}}_i \underline{\mathbf{b}}_i^T \quad (17)$$

If $\underline{\mathbf{M}}$ in Equation (8) is substituted by $\underline{\mathbf{G}}(s)$ then Equation (8) can be rewritten as:

$$\underline{\mathbf{G}}(s) = \sum_{k=1}^r \sigma_k(s) \underline{\mathbf{u}}_k(s) \underline{\mathbf{v}}_k(s)^C \quad (18)$$

If s is near a pole of the system (p_i), then the transfer function of the system from Equation (17) can be simplified as:

$$\underline{\mathbf{G}}(s) \cong \frac{1}{s - p_i} \underline{\mathbf{c}}_i \underline{\mathbf{b}}_i^T \quad (19)$$

since other terms are small enough. For s near to p_i , σ_1 goes to infinity and the other terms can be omitted. So Equation (18) reduces to:

$$\underline{\mathbf{G}}(s) \cong \sigma_1(s) \underline{\mathbf{u}}_1(s) \underline{\mathbf{v}}_1(s)^C \quad (20)$$

As mentioned before, the relative magnitude elements of $\underline{\mathbf{c}}_i$ correspond to the relative observability of output candidates, the relative magnitude elements of $\underline{\mathbf{b}}_i$ correspond to the relative controllability of input candidates and the elements of $\underline{\mathbf{c}}_i \underline{\mathbf{b}}_i^T$ correspond to the residues of λ_i with respect to different input–output pairs. The following lemma with Equations (19) to (20) shows that $\underline{\mathbf{u}}_1(s)$ has information about observability and $\underline{\mathbf{v}}_1(s)$ has information about controllability and $\underline{\mathbf{u}}_1 \underline{\mathbf{v}}_1^C$ gives information about residue of the oscillation mode corresponding to different input–output pairs.

Lemma.

Consider $\underline{\mathbf{c}}$ and $\underline{\mathbf{u}}$ are $p \times 1$ vectors, $\underline{\mathbf{b}}$ and $\underline{\mathbf{v}}$ are $n \times 1$ vectors, and k_1, k_2, k_3 and k_4 are scalars. Then

$$k_1 \underline{\mathbf{c}} \underline{\mathbf{b}}^T = k_2 \underline{\mathbf{u}} \underline{\mathbf{v}}^C \quad (21)$$

implies that

$$\underline{\mathbf{u}} = k_3 \underline{\mathbf{c}} \quad \text{and} \quad \underline{\mathbf{v}}^* = k_4 \underline{\mathbf{b}} \quad (22)$$

(.)^{*} means conjugate. Proof of the lemma is in Appendix A.

6. APPLICATION OF RGA AND SVD IN MULTI-MACHINE POWER SYSTEMS

To use the method based on RGA and SVD to locate PSSs in a MIMO power system, RGA elements are considered in the frequency range from 1 rad/s to 16 rad/s corresponding to the frequency of oscillation. The system has large sensitivity of element-by-element uncertainty for large elements in the RGA matrix. Some generators contribute to each oscillation mode and there is a large interaction among them. Large RGA elements are a measure of interaction, so one can find generators contributing in each oscillation mode through RGA elements. After finding generators contributing in each oscillation mode, the input and output directions and their products lead to the determination of the best locations according to Section 5.

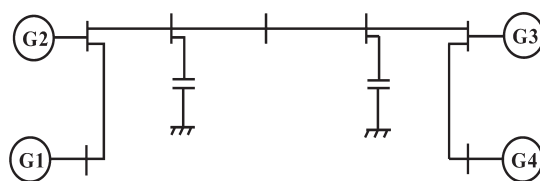


Figure 4. Example of a four-machine power system.

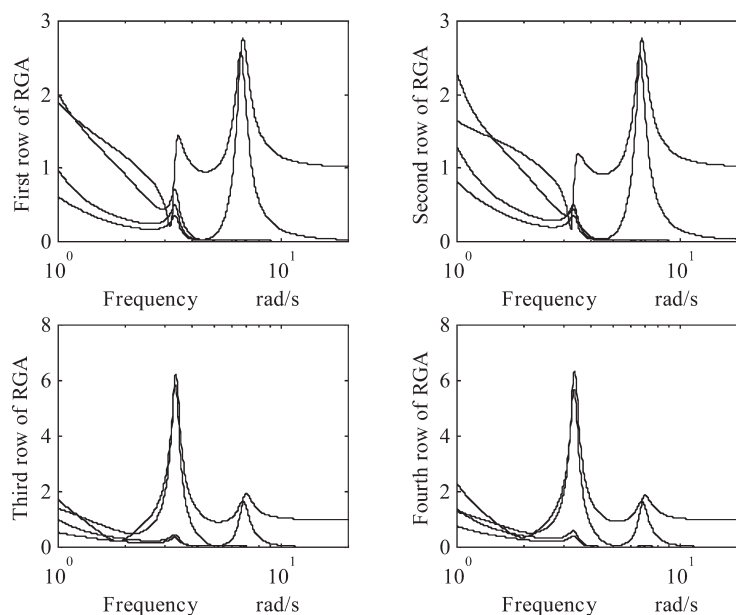


Figure 5. RGA elements of a four-machine system.

6.1. Four-machine system with resonance mode

Using the example of a four-machine system (Figure 4), it is shown in Reference [20] that this system has two oscillation modes very close to each other. It is also illustrated in Reference [20] that in this case the indices according to eigenvector methods do not work correctly and one must make minor variations in some system parameters (inertia of all machines of one area in Reference [20]) to find suitable results for applying PSSs according to the eigenvector methods.

A study has been conducted to examine the applicability of the RGA and SVD methods to such systems with modal resonance. Considering the exciters of generators as inputs and their speeds as outputs, the transfer function of the system is extracted. Elements of RGA versus frequency are shown in Figure 5. It can be seen that there are two peaks in the RGA elements. The absolute value of RGA elements at 3.35 rad/s is:

$$\hat{\mathbf{A}}(j3.35) = \begin{bmatrix} 0.7169 & 1.0937 & 0.3551 & 0.4968 \\ 0.7529 & 0.4311 & 0.3633 & 0.5053 \\ 0.3709 & 0.4676 & 5.8485 & 6.1447 \\ 0.4002 & 0.5991 & 6.2690 & 5.6513 \end{bmatrix}$$

The relative values of RGA elements show that all generators contribute in this mode. The absolute value of RGA at 6.7 rad/s is:

$$\hat{\Delta}(j6.7) = \begin{bmatrix} 2.7723 & 2.4357 & 0.0146 & 0.0198 \\ 2.4054 & 2.7594 & 0.0098 & 0.0180 \\ 0.0351 & 0.0337 & 1.6323 & 1.6771 \\ 0.0370 & 0.0390 & 1.6918 & 1.5789 \end{bmatrix}$$

At this frequency there is interaction only between the sets $\{G_1, G_2\}$ and $\{G_3, G_4\}$. Thus, there are two local oscillation modes corresponding to each set.

For choosing the best input–output pair for improving the damping of inter-area mode p , one must find the SVD of the system at $s = p + \varepsilon$. The SVD of the system at this pole is:

$$\mathbf{G}_{\text{all}} \cong 41.6 \begin{bmatrix} 0.1578 - 0.0578i \\ 0.1117 - 0.0581i \\ -0.6039 - 0.3962i \\ -0.5487 - 0.3648i \end{bmatrix} \begin{bmatrix} 0.4794 \\ 0.4904 + 0.0239i \\ -0.5028 + 0.0004i \\ -0.5251 - 0.0242i \end{bmatrix}^C$$

Absolute values of elements of \mathbf{u}_1 and \mathbf{v}_1 are shown by $\hat{\mathbf{u}}_1$ and $\hat{\mathbf{v}}_1$ correspondingly:

$$\hat{\mathbf{u}}_1 = \begin{bmatrix} 0.1680 \\ 0.1259 \\ 0.7223 \\ 0.6589 \end{bmatrix} \quad \hat{\mathbf{v}}_1 = \begin{bmatrix} 0.4794 \\ 0.4910 \\ 0.5028 \\ 0.5256 \end{bmatrix}$$

$\mathbf{u}_1 \mathbf{v}_1^C$ gives the residue, \mathbf{R} , of the system, the absolute value of \mathbf{R} is shown by $\hat{\mathbf{R}}$

$$\hat{\mathbf{R}} = \begin{bmatrix} 0.0806 & 0.0825 & 0.0845 & 0.0883 \\ 0.0603 & 0.0618 & 0.0633 & 0.0662 \\ 0.3463 & 0.3547 & 0.3632 & 0.3797 \\ 0.3159 & 0.3236 & 0.3313 & 0.3464 \end{bmatrix}$$

The relative magnitude of $\hat{\mathbf{v}}_1$ shows that the exciter of generator four is the best input candidate and the relative magnitude of $\hat{\mathbf{u}}_1$ shows that the speed of generator three is the best measurement signal. The absolute value of residue matrix $\hat{\mathbf{R}}$ considers both controllability and observability and suggests generator three for applying the PSS.

For a study on the local oscillation modes, RGA shows that there are two local modes for sets $\{G_1, G_2\}$ and $\{G_3, G_4\}$. For the local mode of set $\{G_1, G_2\}$ one must extract the transfer function corresponding to these generators. The SVD of this transfer function at $s = p + \varepsilon$ is:

$$\mathbf{G}_{\text{all}} \cong 22.51 \begin{bmatrix} 0.6213 - 0.0422i \\ -0.7807 + 0.0522i \end{bmatrix} \begin{bmatrix} 0.7143 \\ -0.6995 - 0.0236i \end{bmatrix}^C$$

Absolute values of elements of \mathbf{u}_1 and \mathbf{v}_1 are shown by $\hat{\mathbf{u}}_1$ and $\hat{\mathbf{v}}_1$ correspondingly:

$$\hat{\mathbf{u}}_1 = \begin{bmatrix} 0.6227 \\ 0.7825 \end{bmatrix} \quad \hat{\mathbf{v}}_1 = \begin{bmatrix} 0.7143 \\ 0.6999 \end{bmatrix}$$

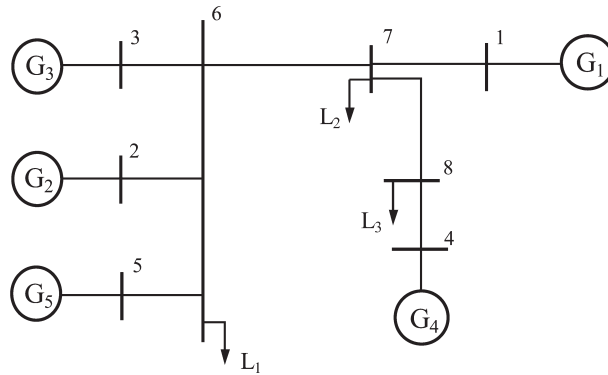


Figure 6. Example of a five-machine power system.

absolute value elements of the residues of the system are:

$$\hat{\mathbf{R}} = \begin{bmatrix} 0.4448 & 0.4358 \\ 0.5589 & 0.5476 \end{bmatrix}$$

The relative magnitude of $\hat{\mathbf{v}}_1$ shows that the exciter of generator one is the best input candidate and the relative magnitude of $\hat{\mathbf{u}}_1$ shows that the speed of generator two is the best measurement signal. The absolute value of residue matrix $\hat{\mathbf{R}}$ suggests generator two for applying PSS. The same procedure for the set $\{G_3, G_4\}$ shows that the exciter of generator four is the best input candidate and the speed of generator four is the best measurement signal. So generator four is the best candidate for applying PSS.

6.2. Five-machine system with multi-mode oscillations

A single line diagram of a five-machine eight-bus system is shown in Figure 6. The parameters of the model and operating conditions are given in Reference [21]. A known signal is applied to the exciter of each generator and both the input signal and the speed of each generator, as the output, are recorded. Using this procedure, a twelfth order transfer function for each output–input pair of the system model is determined. This system has a low damping oscillation mode with frequency of 4 rad/s and all generators are convolving in this mode [18], The SVD of the system at this oscillation mode is:

$$\mathbf{G}_{\text{all}} \cong 101 \begin{bmatrix} -0.1521 + 0.1742i \\ 0.3574 - 0.4489i \\ 0.2422 - 0.3945i \\ -0.2692 + 0.3333i \\ 0.2451 - 0.3992i \end{bmatrix} \begin{bmatrix} 0.2029 \\ -0.8500 - 0.0662i \\ -0.0634 - 0.0015i \\ 0.4736 + 0.0023i \\ -0.0603 - 0.0017i \end{bmatrix}^c$$

The absolute values of elements of \mathbf{u}_1 and \mathbf{v}_1 are shown by $\hat{\mathbf{u}}_1$ and $\hat{\mathbf{v}}_1$ correspondingly:

$$\hat{\mathbf{u}}_1 = \begin{bmatrix} 0.2312 \\ 0.5738 \\ 0.4629 \\ 0.4284 \\ 0.4685 \end{bmatrix} \quad \hat{\mathbf{v}}_1 = \begin{bmatrix} 0.2029 \\ 0.8526 \\ 0.0635 \\ 0.4736 \\ 0.0603 \end{bmatrix}$$

the absolute value elements of the residues of the system are:

$$\hat{\mathbf{R}} = \begin{bmatrix} 0.0469 & 0.1971 & 0.0147 & 0.1095 & 0.0139 \\ 0.1164 & 0.4892 & 0.0364 & 0.2717 & 0.0346 \\ 0.0939 & 0.3946 & 0.0294 & 0.2192 & 0.0279 \\ 0.0869 & 0.3653 & 0.0272 & 0.2029 & 0.0258 \\ 0.0951 & 0.3994 & 0.0297 & 0.2219 & 0.0283 \end{bmatrix}$$

The relative magnitude of $\hat{\mathbf{v}}_1$ shows that the exciter of generator two is the best input candidate, the relative magnitude of $\hat{\mathbf{u}}_1$ shows that the speed of generator two is the best measurement signal. The absolute value of residue matrix $\hat{\mathbf{R}}$ considers both controllability and observability and suggests generator two for applying the PSS. For another oscillation mode with frequency of 6.4 rad/s, generators one and four are in this mode. The SVD of their corresponding transfer function is:

$$\mathbf{G}_{\text{all}} \cong 31 \begin{bmatrix} -0.0599 + 0.7549i \\ 0.0134 - 0.6530i \end{bmatrix} \begin{bmatrix} 0.5845 \\ -0.8078 + 0.0763i \end{bmatrix}^c$$

The absolute values of elements of \mathbf{u}_1 and \mathbf{v}_1 are shown by $\hat{\mathbf{u}}_1$ and $\hat{\mathbf{v}}_1$ correspondingly:

$$\hat{\mathbf{u}}_1 = \begin{bmatrix} 0.7573 \\ 0.6531 \end{bmatrix} \quad \hat{\mathbf{v}}_1 = \begin{bmatrix} 0.5845 \\ 0.8114 \end{bmatrix}$$

the absolute value elements of the residues of the system are:

$$\hat{\mathbf{R}} = \begin{bmatrix} 0.4426 & 0.6144 \\ 0.3817 & 0.5299 \end{bmatrix}$$

The relative magnitude of $\hat{\mathbf{v}}_1$ shows that the exciter of generator one is the best input candidate, the relative magnitude of $\hat{\mathbf{u}}_1$ shows that the speed of generator four is the best measurement signal. The absolute value of residue matrix $\hat{\mathbf{R}}$ considers both controllability and observability and suggests generator four for applying PSS.

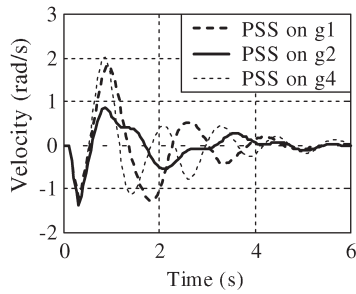
Results of non-linear simulation when one PSS (Equation (23)) is applied on each of the large generators, i.e. 1, 2 and 4 in turn and a 200 ms 3-phase short circuit is applied on bus 3, are shown in Figures 7(a) and (b) and for a short circuit on bus 2 are shown in Figures 7(c) and (d).

$$F(s) = 0.5 \frac{10s}{1 + 10s} \frac{1 + 0.2s}{1 + 0.04s} \frac{1 + 0.2s}{1 + 0.04s} \quad (23)$$

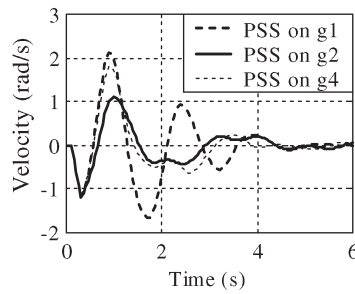
It can be seen that applying PSS on generator two leads to the best performance of the system for the damping of the inter-area mode as determined by the above analysis.

7. CONCLUSIONS

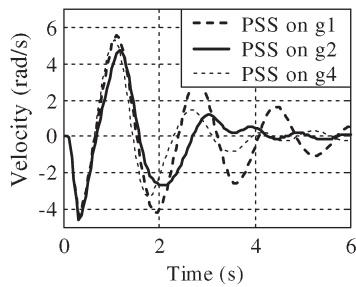
In this paper new measures according to RGA and SVD are introduced and the relationship between the measure according to SVD and the measure according to residues is investigated. The new measure



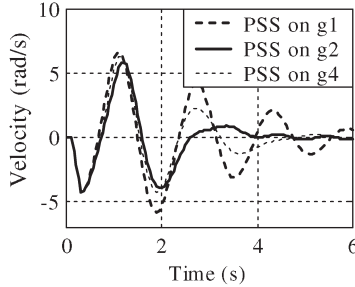
(a) Difference in speed of G_1 and G_2
for short circuit on bus 3



(b) Difference in speed of G_2 and G_4
for short circuit on bus 3



(c) Difference in speed of G_1 and G_2
for short circuit on bus 2



(d) Difference in speed of G_2 and G_4
for short circuit on bus 2

Figure 7. Result for the five-machine system.

can consider controllability and observability of oscillation modes as well as the residue method. This measure only uses the information of the transfer function matrix and can be used to find the best location for applying PSSs. The advantages of the proposed method are:

- No computation involving the right (left) eigenvectors and eigen sensitivity analysis is required.
- This method requires information about the transfer function that can be found from system simulation or modelling.
- There is considerable reduction in the size of the convolved matrices, since it uses only the transfer function of a system and doesn't consider the states of a system.

Test results on power system networks, especially a system with resonance mode, show the applicability of the method for systems with resonance modes.

8. LIST OF SYMBOLS AND ABBREVIATIONS

Symbols

\mathbf{G}	transfer function matrix
g_{ij}	ij -th element of matrix \mathbf{G}
\mathbf{U}	output direction matrix
Σ	singular value matrix
$\hat{\mathbf{u}}_r$	absolute value of r -th output direction
$\hat{\mathbf{v}}_r$	absolute value of r -th input direction
δ	power angle
U_t	terminal voltage
I_t	generator current
\mathbf{G}_{all}	transfer function with all input–output candidates
$\hat{\Lambda}$	absolute value elements of RGA matrix
\mathbf{A}	state matrix
\mathbf{C}	coefficient matrix of output vector
\mathbf{c}_i	observability matrix corresponding to λ_i
\mathbf{R}	residue matrix corresponding to λ_i
$\frac{\varphi_i}{\gamma^*}$	right eigenvector corresponding to λ_i
λ_{ij}	ij -th element of RGA matrix
\mathbf{V}	input direction matrix
\mathbf{u}_r	r -th output direction
\mathbf{v}_r	r -th input direction
σ_r	r -th singular value
ω	speed of generator
P_e	electrical power
$\int (P_e - P_m) dt$	integral of acceleration power
Λ	RGA matrix
Λ_Σ	row sum of RGA matrix
\mathbf{B}	coefficient matrix of input vector
λ_i	i -th eigenvalue
\mathbf{b}_i	controllability matrix corresponding to λ_i
$\hat{\mathbf{R}}$	absolute value elements of residue matrix
ψ_i	left eigenvector corresponding to λ_i

Abbreviations

RGA	Relative Gain Arrays
PRG	Partial Relative Gains
PSS	Power System Stabilizer
Gov	Governor
MIMO	Multi Input Multi Output
SVD	Singular Value Decomposition
CLIN	Closed Loop Interaction Number
Ex	Exciter
AVR	Automatic Voltage Regulator

APPENDIX A

Rewriting Equation (21) by its elements leads to

$$k_1 \begin{bmatrix} c_1 \\ c_2 \\ \cdot \\ \cdot \\ c_p \end{bmatrix} [b_1 b_2 \dots b_n] = k_2 \begin{bmatrix} u_1 \\ u_2 \\ \cdot \\ \cdot \\ u_p \end{bmatrix} [v_1^* v_2^* \dots v_n^*] \quad (\text{A1})$$

where c_i, b_i, u_i and v_i are elements of $\underline{a}, \underline{b}, \underline{u}$ and \underline{v} , respectively. Multiplication of vectors in Equation (A1) leads to:

$$k_1 \begin{bmatrix} c_1 b_1 & c_1 b_2 & \dots & c_1 b_n \\ c_2 b_1 & c_2 b_2 & \dots & c_2 b_n \\ \cdot & \cdot & \dots & \cdot \\ \cdot & \cdot & \dots & \cdot \\ c_p b_1 & c_p b_2 & \dots & c_p b_n \end{bmatrix} = k_2 \begin{bmatrix} u_1 v_1^* & u_1 v_2^* & \dots & u_1 v_n^* \\ u_2 v_1^* & u_2 v_2^* & \dots & u_2 v_n^* \\ \cdot & \cdot & \dots & \cdot \\ \cdot & \cdot & \dots & \cdot \\ u_p v_1^* & u_p v_2^* & \dots & u_p v_n^* \end{bmatrix} \quad (\text{A2})$$

Now comparing elements of the first row of Equation (A2) shows that

$$k_1 c_1 [b_1 b_2 \dots b_n] = k_2 u_1 [v_1^* v_2^* \dots v_n^*] \quad (\text{A3})$$

and comparing elements of the first column of Equation (A2) shows that

$$k_1 b_1 [c_1 c_2 \dots c_p]^T = k_2 v_1^* [u_1 u_2 \dots u_p]^T \quad (\text{A4})$$

Equations (A3) and (A4) directly lead to Equation (22) with $k_3 = k_1 b_1 / k_2 v_1^*$ and $k_4 = k_1 c_1 / k_2 u_1$.

REFERENCES

1. Havre K. Studies on controllability analysis and control structure design. Norwegian University of Science and Technology 1998; Ph.D. Thesis.
2. Foss AS. Critique of chemical process control theory. *AICHE Journal* 1973; **19**:209–214.
3. Skogestad S, Postletwaite I. *Multivariable Feedback Control*, 1st edn. Wiley: New York, 1997.
4. Haggblom KE. Control structure analysis by partial relative gains. *Conference on Decision and Control (IEEE)*, 1997; Vol. 3, pp. 2623–2624.
5. Asgharian R, Karimpour A. Closed loop interaction number (CLIN) as a measure for pairing in decentralized control. *10th Iranian Conference on Electrical Engineering (ICEE)*, University of Tabriz, Tabriz, Iran, 2002; Vol. 3, pp. 229–236.
6. Hsu YY, Chen CL. Identification of optimum location for stabilizer applications using participation factors. *IEE Proceedings: Part C* 1987; **3**:238–244.
7. Zhou EZ, Malik OP, Hope GS. Theory and method for selection of power system stabilizer location. *IEEE Transactions on Energy Conversion* 1991; **6**:170–176.
8. Hamdan AM. An investigation of the significance of singular value decomposition in power system dynamics. *International Journal of Electric Power and Energy Systems* 1999; **6**:417–427.
9. Hamdan AM. Use of SVD for power system stabilizer signal selection. *Electric Machines and Power Systems* 1993; **2**: 229–240.

10. Wang HF, Swift FJ, Li M. Indices for selecting the best location of PSSs or FACTS-based stabilizers in multimachine power systems: a comparative study. *IEE Proceedings: Generation, Transmission and Distribution* 1997; **2**:155–159.
11. Zhang P, Messina AR, Coorick A, Cory BJ. Selection of location and input signals for multiple SVC damping controller in large-scale power systems. *IEEE Power Engineering Society Winter Meeting* 1999; pp. 667–670.
12. Milanovic JV, Duque ACS. The use of relative gain array for optimal placement of PSSs. *IEEE Power Engineering Society Winter Meeting* 2001; pp. 992–996.
13. Castro JC, Araujo CSD. Frequency domain analysis of oscillatory modes in decentralized control systems. *Automatica* 1988; **12**:1647–1653.
14. Limba N, Lima LTG. Determination of suitable locations for power system stabilizers and static var compensators for damping electromechanical oscillations in large-scale power systems. *IEEE Transactions on Power Systems* 1990; **5**:1445–1463.
15. Heniche A, Kamwa I. Control loops selection to damp inter-area oscillations of electrical networks. *IEEE Transactions on Power Systems* 2002; **17**:378–384.
16. Kamwa I, Gerin-Lajoie L. State-space system identification—toward MIMO models for modal analysis and optimization of bulk power systems. *IEEE Transactions on Power Systems* 2000; **15**:326–335.
17. Karimpour A, Asgharian R, Malik OP. PSS design in conjunction with scaling effect. *17th International Power System Conference (PSC)*, Tehran, Iran 2002; Vol. 1, 1–7.
18. Karimpour A, Asgharian R, Malik OP. Determination of PSS location based on singular value decomposition. *International Journal of Electric Power and Energy Systems*, submitted.
19. Yao-nan Yu. *Electric Power System Dynamics*, 1st edn. Academic Press: New York, 1983.
20. Klein M, Rogers GJ, Moorty S, Kundur P. Analytical investigation of factors influencing power system stabilizers performance. *IEEE Transactions on Energy Conversion* 1992; **7**:382–390.
21. Shamsollahi P, Malik OP. Application of neural adaptive power system stabilizer in a multi-machine power system. *IEEE Transactions on Energy Conversion* 1999; **14**:731–736.

AUTHORS' BIOGRAPHIES



Ali Karimpour was born in Mashhad, Iran in 1964. He received his B.Sc. and M.Sc. in Electrical Engineering from Mashhad University, Mashhad, Iran, in 1987 and 1990, respectively. He is a Ph.D. student at Mashhad University and did research at the University of Calgary in 2002 as a visiting student. He is currently working as a lecturer of Electrical Engineering at the Ferdowsi University of Mashhad, Iran.



Rajab Asgharian was born in 1956. He received his M.Sc. from Shiraz (formerly Pahlavi) University in 1980 and his Ph.D. and D.I.C. from Imperial College, University of London, in 1986. He is currently working as an associate professor of Electrical Engineering at the Ferdowsi University of Mashhad, Iran.



O. P. Malik was born in 1937. He graduated in electrical engineering from Delhi Polytechnic, India, in 1952, and obtained the M.E. degree in electrical machine design from the University of Roorkee, India, in 1962. In 1965 he received his Ph.D. degree from the University of London, and his D.I.C. from Imperial College of Science and Technology, London.

He became a Professor at the University of Calgary in 1974 and is now a faculty professor emeritus. He is a Fellow of the Institution of Electrical Engineers (London), and a registered Professor Engineer in the provinces of Alberta and Ontario, Canada.